MVA2002 IAPR Workshop on Machine Vision Applications, Dec. 11 - 13, 2002, Nara - ken New Public Hall, Nara, Japan

2—1

Separating Diffuse and Specular Reflection Components based on Surface Color Ratio and Chromaticity

Robby T.Tan Ko Nishino Katsushi Ikeuchi

Department of Computer Science
The University of Tokyo *

Abstract

A method to separate diffuse and specular reflection components is presented. The method is based on color, particularly on surface color ratio and chromaticity. We define surface color ratio as an invariant to specularity, shading and shadow and use it to detect diffuse pixels. There are three principle steps in our method: diffuse pixels identification, image normalization and reflection components separation. The experimental results show that the proposed method is very accurate and robust for uniform colored dielectric inhomogeneous surfaces under single colored scene illumination.

1 Introduction

Many computer vision algorithms assume perfectly diffuse surfaces and deem specular reflection as an noise or outliers. However, the presence of specularity is inevitable, since in real world there are many dielectric inhomogeneous objects, which have both diffuse and specular reflection components. To properly handle these objects, we need a method to separate the two components robustly.

There are many works on reflection components separation based on color [1] [8] [9] [10]. Early work of using color includes Klinker et al. [8], where they propose a separation algorithm based on the dichromatic reflectance model [11]. The key of their method is to find the distribution of diffuse and specular pixels in a skewed-T shape in RGB color space. However, for many real images, this T shape is hardly extractable due to noise etc. Recently, Lin et al. [10] proposed a method using at least two images of an object taken under different illuminant positions with same viewing direction. By expressing the equation of dichromatic model in terms of spectral basis functions, the combination of the diffuse and specular equations provides a closed form solution to derive the specular component. Their method is applied on a pixel base, hence it is applicable to highly textured surfaces. One drawback is that it requires multiple images of the same object.

Bajscy et al. [1] proposed a method using a three dimensional space composed of lightness, saturation and hue. This method only requires a single image as the input. First, the input image has to be neutralized to pure-white illumination. The neutralization is done using linear basis functions of both illumination spectral energy distribution and surface spectral reflectance, where the weighting factors of illumination basis functions are computed by using a white reference surface captured under the same illumination. After this neutralization, the weighting factors of all pixels of surface reflectance basis functions are projected into a three-dimensional space. In this space, the specular and diffuse reflections are identifiable, as their saturation values are different. This method is more accurate than the method of Klinker et al. [8]. However, there are several weaknesses in this method. First, the use of basis functions to approximate illumination spectral energy distribution is sometimes crude. For uncommon illumination spectral energy distribution, e.g. green illumination, there are no basis functions that can approximate the illumination. Secondly, camera sensitivity data is required to calculate weighting factors of illumination linear basis functions using white reference, and as a result, tedious calibration procedures are required.

The outline of our method can be depicted as Figure 6. The key of our separation method is in the analysis of differences of saturation values between diffuse and specular reflection. Given a single image with uniform surface color taken under single colored illumination, we first group the image pixels based on their surface color ratio values. From each group, we detect the diffuse pixels using the camera noise characteristic. Then, these diffuse pixels are divided by estimated illumination chromaticity, which is derived using a color constancy algorithm. We call this process as normalization. This normalization is also applied to the input image. After computing the normalized diffuse pixels and the normalized image, the separation can be done in a straightforward manner by using what we refer to specular-to-diffuse mechanism. Finally the separated diffuse and specular reflections of normalized image can be renormalized back by multiplying each pixel with the estimated illumination chromaticity.

The rest of the paper is organized as follows. In Section 2, we discuss the dichromatic model of inhomogeneous materials and image color formation. In Section 3, we explain the method in detail, describing the derivation of the theory and the algorithm for separating diffuse and specular reflection components. We provide a brief description of the implementation of the method, experimental results and their evaluations for both synthetic and real images, in Section 4. Finally in Section 5, we offer our conclusions.

*Institute of Industrial Science, The University of Tokyo 4-6-1 Komaba Meguro-ku, Tokyo, JAPAN 153-8505, robby,kon,ki@cvl.iis.u-tokyo.ac.jp

2 Reflection Models

Surface reflection on most inhomogeneous materials can be described with the dichromatic reflection model, which states that the light reflected from an object is a linear combination of diffuse and specular reflections:

$$I(\lambda, \mathbf{x}) = w_d(\mathbf{x}) S_d(\lambda, \mathbf{x}) E(\lambda, \mathbf{x}) + \tilde{w}_s(\mathbf{x}) E(\lambda, \mathbf{x}) \quad (1)$$

where $\mathbf{x} = \{x, y, z\}$, the position of the surface point in a three-dimensional world coordinate system. $w_d(\mathbf{x})$ is the geometrical weighting factor for diffuse reflection. Also $\tilde{w}_s(\mathbf{x}) = w_s(\mathbf{x}) k_s(\mathbf{x})$, where $k_s(\mathbf{x})$ is the scene radiance to surface irradiance ratio of specular surface which is ideally constant w.r.t. wavelength. $w_s(\mathbf{x})$ is geometrical weighting factor for specular reflection. $S_d(\lambda, \mathbf{x})$ is the diffuse surface spectral reflectance function, and $E(\lambda, \mathbf{x})$ is the spectral energy distribution function of the illumination. In this paper we assume that the input is an object with a uniform surface color under a single illumination color, so that the dependence on location $\mathbf{x}$ for surface spectral reflectance and illumination spectral energy distribution can be removed. If the reflected light is captured by a camera, by ignoring camera noise and camera gain, the camera output can be described as:

$$I_c(\bar{\mathbf{x}}) = w_d(\bar{\mathbf{x}}) \int_\Omega S(\lambda) E(\lambda) q_c(\lambda) d\lambda + \tilde{w}_s(\bar{\mathbf{x}}) \int_\Omega E(\lambda) q_c(\lambda) d\lambda \quad (2)$$

where $\bar{\mathbf{x}} = \{s, t\}$, the two dimensional image coordinates, q_c is the three-element-vector of sensor sensitivity and c represents the type of sensors (R, G, and B). The integration is done over the visible spectrum (Ω). Equation (2) can be simplified as:

$$I_c(\bar{\mathbf{x}}) = m_d(\bar{\mathbf{x}}) \Lambda_c + m_s(\bar{\mathbf{x}}) \Gamma_c \quad (3)$$

where $m_d(\bar{\mathbf{x}}) = w_d(\bar{\mathbf{x}}) L(\bar{\mathbf{x}}) k_d$, with $L(\bar{\mathbf{x}})$ is the spectral magnitude of the surface irradiance on a plane perpendicular to the light source direction, k_d is the scene radiance to surface irradiance ratio of diffuse surface. $m_s = \tilde{w}_s(\bar{\mathbf{x}}) L(\bar{\mathbf{x}})$. $\Lambda_c = \int_\Omega s(\lambda) e(\lambda) q_c(\lambda) d\lambda$; with $s(\lambda)$ is the normalized surface reflectance spectral function, $e(\lambda)$ is the normalized illumination spectral energy distribution. $\Gamma_c = \int_\Omega e(\lambda) q_c(\lambda) d\lambda$.

Several researchers in color constancy [5, 14, 10] use narrow band sensor sensitivity assumption in their analysis, where they can use Dirac delta function, $q_c(\lambda) = \delta(\lambda - \lambda_c)$, for the sensitivity. With narrow band assumption equation (2) can be written as,

$$I_c(\bar{\mathbf{x}}) = w_d(\bar{\mathbf{x}}) S(\lambda_c) E(\lambda_c) + \tilde{w}_s(\bar{\mathbf{x}}) E(\lambda_c). \quad (4)$$

The Dirac delta assumption for sensor sensitivity simplifies the image formation equation, while it is an idealization. However, it has been shown that most cameras can be approximated with this assumption [5, 14]. Even when the approximation does not hold, Finlayson et al. [4] and Barnard et al. [2] proposed a method to make it hold, by applying an appropriate change of sensor basis, which is referred to as sensor sharpening.

Now, if we define S_c as the normalized surface color in RGB channels, E_c as the normalized illumination color in RGB channels and $L(\bar{\mathbf{x}})$ as the illuminant magnitude (intensity or brightness), if can rewrite equation (5) as:

$$I_c(\bar{\mathbf{x}}) = w_d(\bar{\mathbf{x}}) k_d S_c L(\bar{\mathbf{x}}) E_c + \tilde{w}_s(\bar{\mathbf{x}}) L(\bar{\mathbf{x}}) E_c. \quad (5)$$

This equation can be simply described as,

$$I_c(\bar{\mathbf{x}}) = m_d(\bar{\mathbf{x}}) S_c E_c + m_s(\bar{\mathbf{x}}) E_c. \quad (6)$$

Hence we have two versions of dichromatic model, i.e.: dichromatic model without narrow band assumption (3) and dichromatic model with narrow band assumption (6).

From color constancy algorithms, we can estimate the illumination chromaticity. The estimated illumination chromaticity will be $\psi_c = n \int_\Omega e(\lambda) q_c(\lambda) d\lambda$, where the value of n is a positive real number ($0 < n \leq 1$). In fact, the exact value of n is unknown, as the magnitude of incident light cannot be recovered with current color constancy algorithms. Fortunately, this value is not necessary, because we only require the ratio of illumination color. Then, using ψ_c can normalize equation (3) w.r.t. the illumination color as:

$$\tilde{I}_c(\bar{\mathbf{x}}) = \tilde{m}_d(\bar{\mathbf{x}}) \tilde{\Lambda}_c(\bar{\mathbf{x}}) + \tilde{m}_s(\bar{\mathbf{x}}) \quad (7)$$

where $\tilde{I}_c(\bar{\mathbf{x}}) = \frac{I_c(\bar{\mathbf{x}})}{\psi_c}$; $\tilde{\Lambda}_c(\bar{\mathbf{x}}) = \frac{\Lambda_c(\bar{\mathbf{x}})}{\int_\Omega e(\lambda) q_c(\lambda) d\lambda}$; $\tilde{m}_d = \frac{m_d}{n}$; $\tilde{m}_s = \frac{m_s}{n}$. Equation (7) shows that the specular reflection component becomes pure-white color.

An alternative method to obtain pure white color of specular reflection component is using narrow band sensor sensitivity assumption. Finlayson [5] developed a color constancy method based on the assumption by directly dividing the input image with normalized illumination color to discount the illumination color. Then, based on the same assumption, we can also normalize equation (6) as:

$$\tilde{I}_c(\bar{\mathbf{x}}) = \tilde{m}_d(\bar{\mathbf{x}}) S_c + \tilde{m}_s(\bar{\mathbf{x}}). \quad (8)$$

Of course, if it is allowed, we can always use an image of a white reference surface captured under the illumination whose color is to be estimated to obtain a robust estimate of the illuminant color. This will improve the result of separation, particularly for an image with high intensity of specular pixels as we will see later.

3 Separation Method

3.1 Chromaticity and Problem Definition

Following Wyszecki et al. [15], we define chromaticity for a normalized image as:

$$\tilde{c}(\bar{\mathbf{x}}) = \frac{\tilde{I}_c(\bar{\mathbf{x}})}{\Sigma \tilde{I}_i(\bar{\mathbf{x}})} \quad (9)$$

where $\Sigma \tilde{I}_i(\bar{\mathbf{x}}) = \tilde{I}_r(\bar{\mathbf{x}}) + \tilde{I}_g(\bar{\mathbf{x}}) + \tilde{I}_b(\bar{\mathbf{x}})$. For a uniformly colored surface lit with a single colored illumination, the chromaticity values of diffuse regions will be constant, regardless of the variance of $\tilde{m}_d(\bar{\mathbf{x}})$. In constrast, the chromaticity values of specular regions will vary with regards to the variance of $\tilde{m}_s(\bar{\mathbf{x}})$. Figure 2.a shows the projection of diffuse and specular

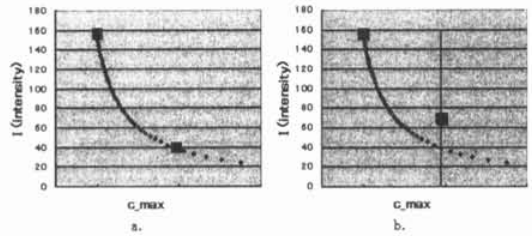

Figure 1: Specular-to-diffuse mechanism, a. the two pixels have same diffuse component, b. the two pixels have different diffuse component

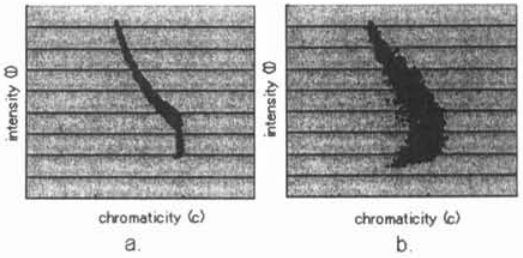

Figure 2: a. The projection of synthetic image pixel into chromaticity-intensity space. b. The projection of real image pixel into chromaticity-intensity space.

regions in $c_{max} - I$ space, where $\tilde{c}_{max}(\bar{\mathbf{x}}) = \frac{\tilde{I}_{max}(\bar{\mathbf{x}})}{\Sigma \tilde{I}_i(\bar{\mathbf{x}})}$; $\tilde{I}_{max}(\bar{\mathbf{x}}) = max[\tilde{I}_r(\bar{\mathbf{x}}), \tilde{I}_g(\bar{\mathbf{x}}), \tilde{I}_b(\bar{\mathbf{x}})]$ and $I(\bar{\mathbf{x}}) = \Sigma \tilde{I}_i(\bar{\mathbf{x}})$. As can be observed in the figure, the diffuse regions form a vertical line, while the specular regions form a curve line cluster. This different characteristic of diffuse and specular regions will lead us to obtain the specular reflection component as well as the diffuse reflection component. The detail is as follows:

If there are two pixels, a specular pixel ($\tilde{I}_{c-spec}$) and a diffuse pixel ($\tilde{I}_{c-diff}$), with the same values of diffuse reflection component ($\tilde{m}_d \tilde{\Lambda}_c$), then by projecting them into $c_{max} - I$ space, we will find that the diffuse point is located at the right side of the specular point. In Figure 1.a, these two points are depicted by square points. If we subtract all channels of the specular pixel intensity ($\tilde{I}_{c-spec}$) with a small positive real number (ϵ): $\tilde{I}_c^1 = \tilde{I}_{c-spec} - \epsilon$, and project the subtracted pixel into the space, then the point will be located near the original specular point. Moreover, if the subtraction is applied iteratively and infinitely by increasing the subtracting number linearly, as: $\tilde{I}_c^i = \tilde{I}_{c-spec} - (\epsilon \times i)$, where i is the natural number denoting count number of iterative looping, the projection of the subtracted pixels will form a curve line that pass through the diffuse point, as depicted in Figure 1.a.

A point in the curve line that lies on top of the diffuse point has $\tilde{m}_s = 0$ and its subtracting number $(\epsilon * i)$ equals to $\tilde{m}_s$ of the original specular pixel. This means, the task of estimating the specular component of the original specular pixel is completed, as we have obtained the value of the specular component ($\tilde{m}_s = \epsilon \times i$). However, this happens if $\tilde{m}_d \tilde{\Lambda}_c$ of both pixels are the same. Otherwise, the curve line will not pass through the point of the diffuse pixel. To solve this case, we create a vertical line crossing the diffuse point, as shown in Figure 1.b. This vertical line will be intersected by the curve line at a certain point, which indicates $\tilde{m}_s = 0$. Then, using the same mechanism of subtraction, $\tilde{m}_s$ of the specular pixel can be obtained. We call this mechanism as specular-to-diffuse mechanism. This mechanism requires a camera that has linear outputs for each color channel.

Therefore, based on the specular-to-diffuse mechanism, the problem of reflection components separation can be defined as: how to identify the diffuse pixels (or c_{max} of the diffuse pixels) from given both specular and diffuse pixels of uniform surface color under a single illumination color. This implies that we need pixels that have only diffuse reflection to accomplish reflection components separation using color.

For synthetic images, which have no noise, the separation problem can be solved easily. As shown in Figure 2.a, using the definition c_{max}, the diffuse points will always be located at the right most of the point cloud. Unfortunately, for real images, the diffuse points are not always at the most right side (Figure 2.b). This is due to imaging noises. Therefore, to robustly obtain the diffuse chromaticity, we must include noise in our analysis. We will focus on the algorithm to accomplish this in the following sections.

Chromaticity is usually used to specify colors in two-dimensional space (chromaticity space). A point in chromaticity space represents the values of both hue and saturation. Several researchers [3, 1] have shown the correlation of specularity, hue and saturation. For a uniform color object under pure-white illumination, the hue values of the specular and diffuse reflections are the same, but their saturation values are different. This difference is due to the intensity variation of specular reflection components. On the other hand, diffuse reflections have constant saturation values. Therefore, saturation becomes important for the separation, because by knowing the saturation value of diffuse pixels of a uniform surface color we can infer the values of the specular component. In this paper we describe the saturation in the context of one-dimensional chromaticity.

3.2 Surface Color Ratio

We define surface color ratio as:

$$u = \frac{I_r + I_b - 2I_g}{I_g + I_b - 2I_r} \tag{10}$$

the location parameter $\bar{\mathbf{x}}$ is removed, since we work on each pixel independently. If $\Gamma_r = \Gamma_g = \Gamma_b$ in equation (3), then u can be expressed as:

$$u = \frac{\Lambda_r + \Lambda_b - \Lambda_g}{\Lambda_g + \Lambda_b - \Lambda_r} \tag{11}$$

Or, using narrow band assumption from equation (6) with $E_r = E_g = E_b$, we obtain:

$$u = \frac{S_r + S_b - 2S_g}{S_g + S_b - 2S_r} \tag{12}$$

We call u as surface color ratio, because as shown in equation (12), u is a function of only the surface color,

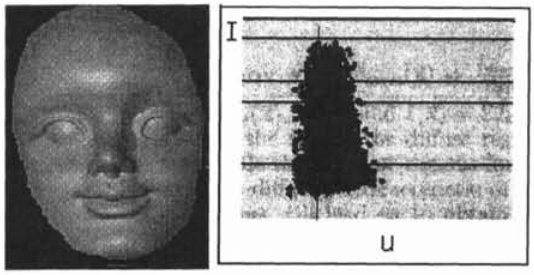

Figure 3: (a). real input image (b). The projection of the pixels of Figure 3.a into u-intensity

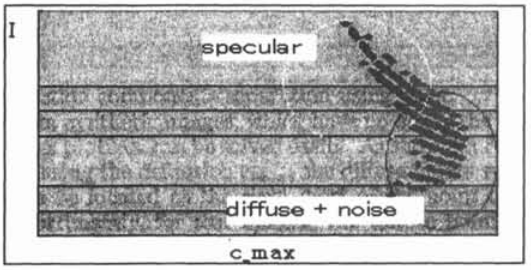

Figure 4: Result of plotting pixels obtained from one straight line in u-intensity space (vertical line in Figure 3.b) into $c_{max} - I$ space.

An important property of u is its invariance property against shadows, shading and specularity. The invariance against shadow is fulfilled if the ambient illumination has the same spectral energy distribution to the direct illumination [6]. For the sake of generality of our discussion (without assuming narrow band sensor sensitivity), in the subsequent explanations, we will use equation (11) instead of equation (12).

Using u in equation (11), we define a two-dimensional space, $u - I$ space, with u as x-axis and I $(= I_r + I_g + I_b)$ as y-axes. By projecting each pixel of a real image into this space, we obtain a cloud of points as shown in Figure 3.b. Ideally, if the surface color is perfectly unique and there is no noise from the camera, we should observe only a straight line in this space. However, as it can be seen in Figure 3, this does not hold for real images. This is mainly due to the slight variation of surface color and illumination color, which are insensible to human eyes, as well as the noise produced through the camera sensing process (camera noise). In our analysis we assume that the illumination color variance is very small, so that it can be neglected.

By considering the camera noise, equation (3) becomes:

$$I_c(\bar{\mathbf{x}}) = \Big[m_d(\bar{\mathbf{x}})\Lambda_c + m_s(\bar{\mathbf{x}})\Gamma_c\Big]\sigma_c(\bar{\mathbf{x}}) + \phi_c(\bar{\mathbf{x}}) \quad (13)$$

where $\sigma_c(\bar{\mathbf{x}})$ and $\phi_c(\bar{\mathbf{x}})$ are the first and second camera noise in the three sensor channels, respectively.

In section 3.1 we have assumed that the camera has linear outputs for each channel. It implies that the noise of each channel is also linear, or at least approximately linear. Therefore, we can set $\sigma_r(\bar{\mathbf{x}}) \approx \sigma_g(\bar{\mathbf{x}}) \approx \sigma_b(\bar{\mathbf{x}})$ and $\phi_r(\bar{\mathbf{x}}) \approx \phi_g(\bar{\mathbf{x}}) \approx \phi_b(\bar{\mathbf{x}})$. These two types of camera noise depend on the position of the image $\bar{\mathbf{x}}$, indicating that the noise can be different for each location in the image. Noise model in equation (13) is the simplification of more complex model proposed by Healey et al. [7].

If $\Gamma_r = \Gamma_g = \Gamma_b$, then the definition of u becomes:

$$\begin{aligned} u \;=\; & \big\{m_d(\Lambda_r\sigma_r + \Lambda_b\sigma_b - 2\Lambda_g\sigma_g) \quad (14)\\ & +m_s\Gamma(\sigma_r + \sigma_b - 2\sigma_g) + (\phi_r + \phi_b - 2\phi_g)\big\}\Big/ \\ & \big\{m_d(\Lambda_g\sigma_g + \Lambda_b\sigma_b - 2\Lambda_r\sigma_r) + \\ & +m_s\Gamma(\sigma_g + \sigma_b - 2\sigma_r) + (\phi_g + \phi_b - 2\phi_r)\big\} \end{aligned}$$

If we look at two pixels that follow equation (14), we can consider several cases as follows:

1. if $\Lambda_c^1 \neq \Lambda_c^2$, then $u^1 \neq u^2$
2. if $\Lambda_c^1 = \Lambda_c^2$ and $\sigma_c^1 \neq \sigma_c^2$, then $u^1 \neq u^2$
3. if $\Lambda_c^1 = \Lambda_c^2$ and $\sigma_c^1 = \sigma_c^2$ and $\phi_c^1 = \phi_c^2$, then $u^1 = u^2$
4. By defining $\Delta_g = \phi_r + \phi_b - 2\phi_g$ and $\Delta_r = \phi_g + \phi_b - 2\phi_r$, if $\Lambda_c^1 = \Lambda_c^2$ and $\sigma_c^1 = \sigma_c^2$ and $\phi_c^1 \neq \phi_c^2$ and $\Delta_g^1 \neq \Delta_g^2$ and $\Delta_r^1 \neq \Delta_r^2$, then $u^1 \neq u^2$
5. if $\Lambda_c^1 = \Lambda_c^2$ and $\sigma_c^1 = \sigma_c^2$ and $\phi_c^1 \neq \phi_c^2$ and $\Delta_g^1 = \Delta_g^2$ and $\Delta_r^1 = \Delta_r^2$, then $u^1 = u^2$.

Case 1 is caused by non-uniformity of surface spectral reflectance and illumination spectral power distribution, even though human eyes percept it as a uniform surface color. Case 2 and case 4 are prompted by the first (σ_c) and second (ϕ_c) types of noises, respectively. All of these cases (1, 2 and 4) make the u values vary. Case 3 and case 5 will produce the same values of u, but if we project the two pixels into $c_{max} - I$ space, we will obtain a different characteristic. In case 3, the chromaticity values of the two pixels will be the same. While in case 5, the pixels will give different values of chromaticity, and make the diffuse pixels behave like specular pixels: $I_{c-diff}(\bar{\mathbf{x}}) = m_d(\bar{\mathbf{x}})\Lambda_c\sigma_c(\bar{\mathbf{x}}) + \phi_c(\bar{\mathbf{x}})$; where the values of $\phi_c(\bar{\mathbf{x}})$ vary. Furthermore, because in case 5 $(\Delta_g^1 = \Delta_g^2)$, $(\Delta_r^1 = \Delta_r^2)$ and $(\phi_r(\bar{\mathbf{x}}) \approx \phi_g(\bar{\mathbf{x}}) \approx \phi_b(\bar{\mathbf{x}}))$, then in each group of u, there are many pixels that $\phi_r(\bar{\mathbf{x}}) = \phi_g(\bar{\mathbf{x}}) = \phi_b(\bar{\mathbf{x}})$. It is like specular pixels under pure-white illumination.

Figure 4 shows a projection of pixels in a group of u into $c_{max} - I$ space. Ideally, without the existence of the camera noise (case 5), the diffuse points should form a single vertical line with the same value of chromaticity. The occurrence of curve lines is due to the variance of the second noise values spatially, or formally it can be written as: $I_{c-diff}(\bar{\mathbf{x}}) = m_d(\bar{\mathbf{x}})\Lambda_c\sigma_c(\bar{\mathbf{x}}) + \phi_c(\bar{\mathbf{x}})$. It also indicates that for each curve line, there is a single value of diffuse component $m_d(\bar{\mathbf{x}})\Lambda_c\sigma_c(\bar{\mathbf{x}})$, with $\phi_c(\bar{\mathbf{x}})$varies.

Therefore, our surface color ratio and chromaticity is like filters that can separate the two types of camera noise. This separation of noise is useful because, from the second type of camera noise we can identify diffuse pixels.

3.3 Diffuse Pixels Identification

In the previous section, we have shown the characteristic of diffuse pixels that behave like specular pix-

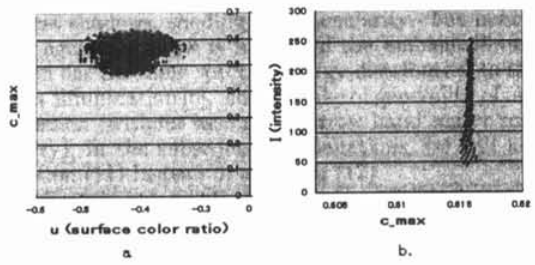

Figure 5: a. Diffuse candidates amongst other pixels in $u - c_{max}$ space, brighter points represent diffuse candidates. b. The c_{max} values of all pixels after separation, these points are identical with points of diffuse component

els with the assumption that the specular components have the same color for each channel ($\Gamma_r = \Gamma_g = \Gamma_b$). For more general cases, we consider an arbitrary color of illumination. Under colored illumination, we cannot assume that the specular components have the same color or chromaticity for each channel. In these cases, the specular pixels will behave differently in $u-I$ space and $c_{max} - I$ space from explanation in Section 3.2. Fortunately, colored illumination in any way does not affect the characteristics of the second type of noise (ϕ_c) of diffuse pixels, so that the diffuse pixels still have the same characteristics as has been explained. This happens because, the noise is independent from illumination color ($E(\lambda)$) and camera sensitivity ($q_c(\lambda)$). Consequently, even in an arbitrary illumination where ($\Gamma_r \neq \Gamma_g \neq \Gamma_b$), diffuse pixels with the same u form a curve line in $c_{max} - I$ space.

Therefore, the identification of diffuse pixels is identical to finding the diffuse curve lines in $c_{max} - I$ space for each group of u. To avoid being trapped in specular pixels which in certain cases have $\Gamma_r = \Gamma_g = \Gamma_b$, we chose the lowest intensity amongst the points in the curve line as candidate diffuse points. Thus, for each u we have several candidates, depending on the number of the curve line inside u. Figure 5.a shows the diffuse candidates in $u - c_{max}$ space.

3.4 Diffuse-Specular Separation

Having obtained the diffuse pixels of arbitrary illumination, we normalize the diffuse pixels as well as all pixels of the input image. The normalization is done simply using equation (7). The values of c_{max} of the diffuse pixels vary depending on the first type of noise and slight variances of surface color, as shown in Figure 5.a. To find a single c_{max} value of diffuse points, we use histogram analysis to find the largest count and use it as diffuse c_{max}. Then, we can separate the diffuse and specular component using specular-to-diffuse mechanism explained in subsection 3.1. Figure 5.b shows the points in $c_{max} - I$ space after separation process. These points represent the diffuse components of the input image.

Finally, we re-normalize the specular and diffuse component value by multiplying them with the estimated illumination chromaticity.

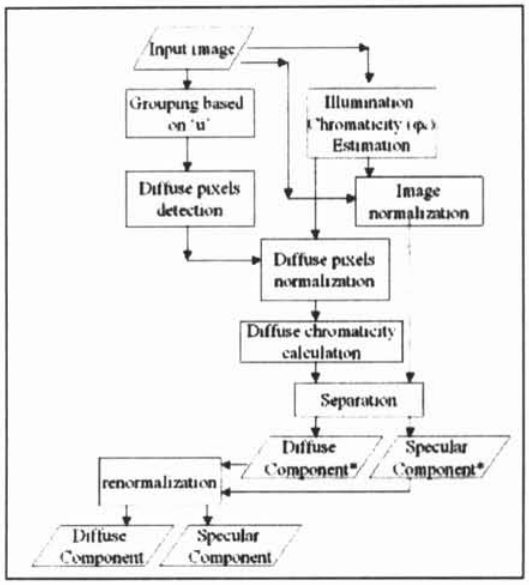

Figure 6: Flowchart of the proposed method, symbol (*) means normalized diffuse and specular components

4 Experimental Results

In this section we first briefly describe the implementation of the proposed method, and then show several experimental results.

Figure 6 shows the flowchart of the method. First, the pixels of an input image is grouped based on the value of u. For each group of u, we identify the diffuse pixels. Then, these diffuse pixels are normalized using estimated illumination chromaticity. The normalization is also applied to all pixels of the input image. From the normalized diffuse pixels, we calculate the diffuse chromaticity using histogram analysis. Having known the diffuse chromaticity, the normalized image can be separated using specular-to-diffuse mechanism. The separation yields normalized diffuse and specular components. To obtain the actual components, we renormalized back by multiplying with the estimated illumination chromaticity.

We have conducted several tests on both synthetic and real images. Synthetic images used in our experiments were rendered using the Torrance-Sparrow reflection model [13]. Real images were taken using a SONY DXC-9000, a progressive 3 CCD digital camera. To estimate illumination chromaticity, we used color constancy algorithm proposed by Tan et al. [12], and alternatively we also used a white reference from Photo Research Reflectance Standard model: SRS-3 S/N.983901. As target objects, we use convex objects to avoid interreflection. For complete results in color, please visit: www.cvl.u-tokyo.ac.jp/~robby/mva02/results.html

Figure 7.a shows a synthetic image with a green surface under incandescent light (2800 K). The separation of the diffuse and specular reflection components are shown in Figure 7.b and 7.c respectively. Figure 8.a shows a head model under two incandescent light sources. The specularity of this head model is low.

Figure 7: Separation results: a. Synthetic input image b. diffuse reflection component c. specular reflection component

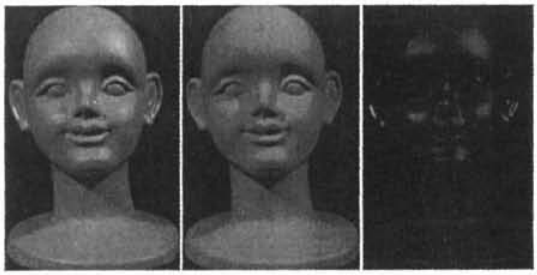

Figure 8: Separation results: a. Real input image b. diffuse reflection component c. specular reflection component

The results of separation can be observed in Figure 8.b and 8.c. Figure 9.a shows a green sandal with high specularity under incandescent light. The results of separation can be observed in Figure 9.b and 9.c.

5 Conclusion

We have proposed a new method to separate diffuse and specular reflection component. The main insight of our separation method is on the analysis of the difference of saturation values between diffuse and specular reflection. Along with the method we also proposed surface color ratio that is invariant against shadows, shading and specularity. Furthermore, we also explained the effects of camera noises in relation with the surface color ratio. As future works we plan to exhance our framework to handle textured surfaces.

References

[1] R. Bajscy, S.W. Lee, and A. Leonardis. Detection of diffuse and specular interface reflections by color image segmentation. *International Journal of Computer Vision*, 17(3):249–272, 1996.

[2] K. Barnard, F. Ciurea, and B. Funt. Sensor sharpening for computational color constancy. *Journal of Optics Society of America A.*, 18(11):2728–2743, 2001.

[3] M. D'Zmura and P. Lennie. Mechanism of color constancy. *Journal of Optics Society of America A.*, 3(10):1162–1672, 1986.

[4] G.D. Finlayson, M.S. Drew, and B.V. Funt. Spectral sharpening sensor transformations for improved color constancy. *Journal of Optics Society of America A.*, 11(10):1162–1672, 1994.

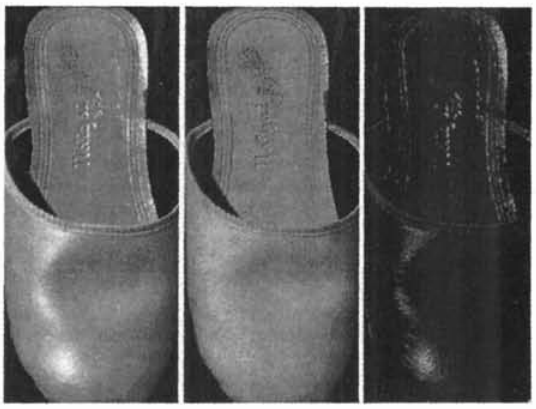

Figure 9: Separation results: a. Real input image, b. diffuse reflection component, small error in the left-top of the sandal is due to saturated intensity of the input image, c. specular reflection component

[5] G.D. Finlayson and S.D.Hordley. Color constancy at a pixel. *Journal of Optics Society of America A.*, 18(2):253–264, 2001.

[6] R. Gershon, A.D. Jepson, and J.K. Tsotsos. Ambient illumination and the determination of material changes. *Journal of Optics Society of America A.*, 3(10):1700–1707, 1986.

[7] G. Healey and R. Kondepudy. Radiometric ccd camera calibration and noise estimation. *IEEE Trans. on Pattern Analysis and Machine Intelligence*, 16(3):267–276, 1994.

[8] G.J. Klinker, S.A. Shafer, and T. Kanade. The measurement of highlights in color images. *International Journal of Computer Vision*, 2:7–32, 1990.

[9] S.W. Lee and R. Bajcsy. Detection of specularity using color and multiple views. *Image and Vision Computing*, 10:643–653, 1990.

[10] S. Lin and H.Y. Shum. Separation of diffuse and specular reflection in color images. In *Conference on Computer Vision and Pattern Recognition*, 2001.

[11] S. Shafer. Using color to separate reflection components. *Color Research and Applications*, 10, 1985.

[12] R. T. Tan, K. Nishino, and K. Ikeuchi. Illumination chromaticity estimation from highlights through inverse intensity-chromaticity space. *On submission*, 2002.

[13] K.E. Torrance and E.M. Sparrow. Theory for off-specular reflection from roughened surfaces. *Journal of Optics Society of America*, 57, 1966.

[14] J.A. Worthey and M.H. Brill. Heuristic analysis of von kries color constancy. *Journal of Optics Society of America A.*, 3(10):1708–1712, 1986.

[15] G. Wyszecki and W.S. Stiles. *Color Science: Concept and Methods, Quantitative Data and Formulae.* Wiley Inter-Science, second edition, 1982.